

# Supporting Information

Marmottant et al. 10.1073/pnas.0902085106

## SI Text

**Cell Viability and Displacements.** Two-photon microscopy provides a means to visualize the shape of fluorescent cells deeply inside aggregates. We demonstrate here that the soluble dye sulforhodamine B (SRB) injected at a concentration of 8  $\mu\text{g}/\text{mL}$  in the culture medium quickly diffuses inside aggregates and stains the intercellular space with an intensity comparable with the SRB present outside of the aggregates. The cell membrane of dead cells becomes permeable to SRB (1), as confirmed by experiments showing that photodamaged cells submitted to a high laser power (700 mW) are completely filled with the dye (data not shown). Fig. S1 shows the middle plane of a F9 aggregate before (A) and during successive compressions of 27% (B) and 57% (C). At the start, the aggregate presents a few very bright dots, often smaller than intact cells. We believe these bright spots are fragments of cells, dead before the beginning of the experiment. Their number does not increase after successive compressions. We therefore conclude that up to at least a 57% compression rate, compression does not lead to the destruction of cells within the aggregate. Movie S1 shows a time series of two-photon microscopy images at the middle plane of the same aggregate just after a 27% compression. Images are taken every minute during 15 min, which is larger than the usual force relaxation period in Fig. S3. Although the aggregate's external boundary is mostly fixed during this relaxation period, cells inside it are clearly actively moving, changing neighbors either in the same plane or from one plane to the other (i.e., some cells are disappearing, others are appearing during that sequence, see the cell inside the circle on the first frame). These qualitative experiments clearly validate the assumptions of our model: that cells are relaxing some of their stress by changing neighbors.

**Monitoring Aggregate Shape.** The aggregate profile during or after compression is recorded with a stereomicroscope (MZ16 binocular, Leica) on a camera (A686M; Pixelink). The lighting is adjusted by a KL 1500 LCD (Leica) through flexible tubes. The whole setup is controlled with Labview (National Instruments), and image analysis is performed with Matlab (The MathWorks) and ImageJ (National Institutes of Health, Bethesda).

**Fusion of Aggregates.** For viscous liquids, various simple geometries are available to estimate (from the analysis of aggregate shape relaxation kinetics) the ratio of the surface tension  $\sigma$  to the viscosity  $\eta^*$ . Ellipticity during the rounding up of elliptical aggregates follows an exponential law with a time characteristic of the surface tension-driven rounding of a liquid,  $T_{\text{Liq}} = \eta^* R_F / \sigma$ , where  $R_F$  is the final aggregate radius (2, 3). When two identical viscous drops of radius  $R_0$  are placed in contact, they slowly fuse together (Fig. S2A and B). The initial regime of such fusion may

be described by  $X^2 = tR_0 \sigma / \eta^*$ , where  $X$  is the radius of the circle of contact between both aggregates, and  $t$  is the time. In the original work by Frenkel (4), there was a mistake about incompressibility, detected by Eshelby (page 806 of the discussion of ref. 5), who removed the extra prefactor  $2/3$  on the right-hand side. We also found a calculus error on the line above Frenkel's equation (7) and removed an extra prefactor  $1/\pi$ . Our corrected formula therefore does not contain any numerical prefactor. This is consistent with a more extensive calculation of the fusion process at large times (6).

In Fig. S2C, we measure the radius of contact  $X$  for three different F9 aggregates and plot  $X^2$  versus  $R_0 t$ . The result is fitted by a straight line with the same slope for the three aggregates,  $\sigma/\eta^* \approx 0.68 \mu\text{m}/\text{min}$ . With  $\sigma \approx 5 \text{ mN}/\text{m}$  (7), we estimate  $\eta^* = 4.4 \cdot 10^5 \text{ Pa}\cdot\text{s}$ . With a typical aggregate radius  $R_F = 250 \mu\text{m}$ , we estimate the characteristic time as  $T_{\text{Liq}} \approx 6 \text{ h}$ .

**Model.** In Eq. 1, the pressure  $p$  is defined as the isotropic part of the internal stresses (trace of the stress tensor, i.e., sum of diagonal components). The normal stress  $\tau$  is a nonisotropic part of stresses (normal part of the deviatoric stress tensor, i.e., difference in diagonal components). For symmetry reasons, we do not consider the shear stress (off-diagonal component). The study of  $\tau$  is thus treated as a scalar problem.

**Relaxation After Compression.** For F9 mouse embryonic cell aggregates, Fig. S3 shows the height relaxation after a prolonged compression (duration  $t_{\text{comp}}$ ), followed by a sudden free decompression (at time taken as  $t = 0$ ). All curves show an initial fast relaxation  $\approx 10^2 \text{ s}$ . The aggregate does not recover completely its initial shape during a recording time of  $\approx 30 \text{ min}$ . The compression has thus promoted irreversible, plastic-like deformations. To recover the initial shape, it is necessary to wait a much longer time, corresponding to the surface tension driven rounding time ( $T_{\text{Liq}} = 6 \text{ h}$ , Fig. S2).

When successive compressions with the same compression time and the same initial relative deformation are applied to an aggregate, plasticity progressively accumulates (Fig. S3A). The relaxation kinetics appear very similar when plotted by using, as a reference height for each compressed aggregate, the final height of the previous step (i.e., relative deformation, Fig. S3B) rather than the initial aggregate height. The viscoelastic response of the aggregate is therefore independent of its history: Cells release their stress between two compressions.

The higher or the longer the compression step, the larger the remaining plasticity at any time. In particular, the remnant plastic deformation after 440 s in the case of Fig. S3C corresponds to  $\varepsilon_{\text{abs}}(0) \approx 0.47$  and  $t_{\text{comp}} = 10 \text{ min}$ , which is for instance  $\varepsilon_{\text{plastic}} = 10\%$  (compared with  $\varepsilon_{\text{plastic}} = 3\%$  for  $\varepsilon_{\text{abs}}(0) \approx 0.15$  and  $t_{\text{comp}} = 1 \text{ min}$ , Fig. S3A).

1. Ricard C, Vial JC, Douady J, van der Sanden B (2007) In vivo imaging of elastic fibers using sulforhodamine B. *J Biomed Opt* 12:064017.
2. Gordon R, Goel NS, Steinberg MS, Wiseman LL (1972) A rheological mechanism sufficient to explain the kinetics of cell sorting. *J Theor Biol* 37:43–73.
3. Mombach JCM, et al. (2005) Rounding of aggregates of biological cells: Experiments and simulations. *Physica A* 352:525–534.

4. Frenkel J (1945) Viscous flow of crystalline bodies. *J Phys* 9:385–391.
5. Shaler AJ (1949) Seminar on the kinetics of sintering. *Metals Trans* 185:796–813.
6. Pokluda O, Bellehumeur CT, Machopoulos J (1997) Modification of Frenkel's model for sintering. *AIChE J* 43:3253–3256.
7. Mgharbel A, Delanoë-Ayari H, Rieu, J-P (2009) Measuring accurately liquid and tissue surface tension with a compression plate tensiometer. *HFSP J* 3:213–221.

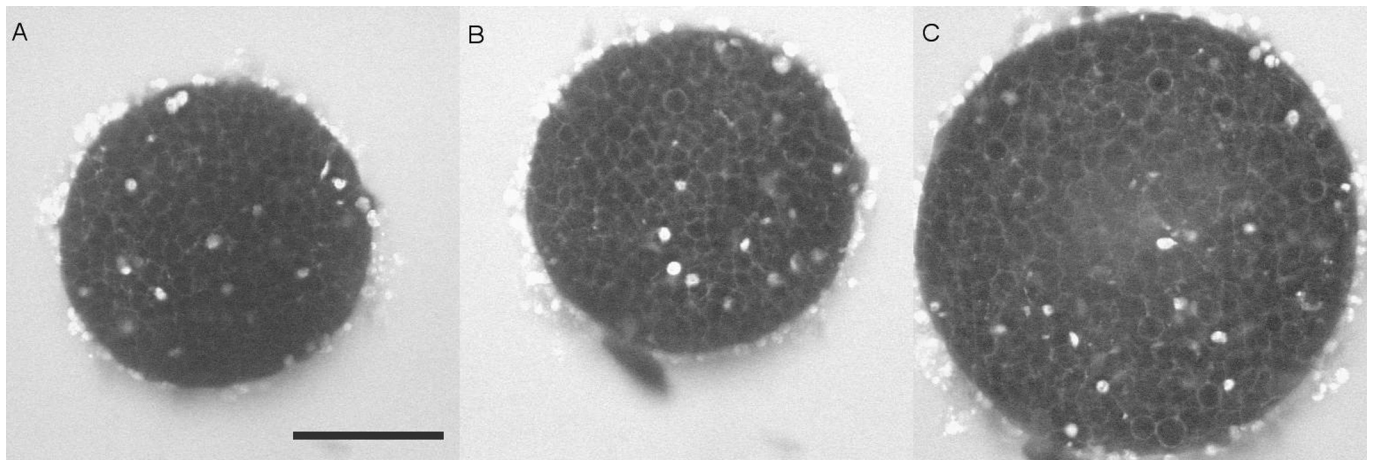


**Fig. S1.** Two-photon microscopy images of the middle plane of a F9 aggregate compressed between parallel plates at successive compression rates of 0% (A), 27% as in Fig. 1 A (B), and 57% (C). Images were acquired 2 min after each compression. The extracellular space is stained with the freely diffusible sulforhodamine B dye. (Scale bar, 100  $\mu\text{m}$ .)





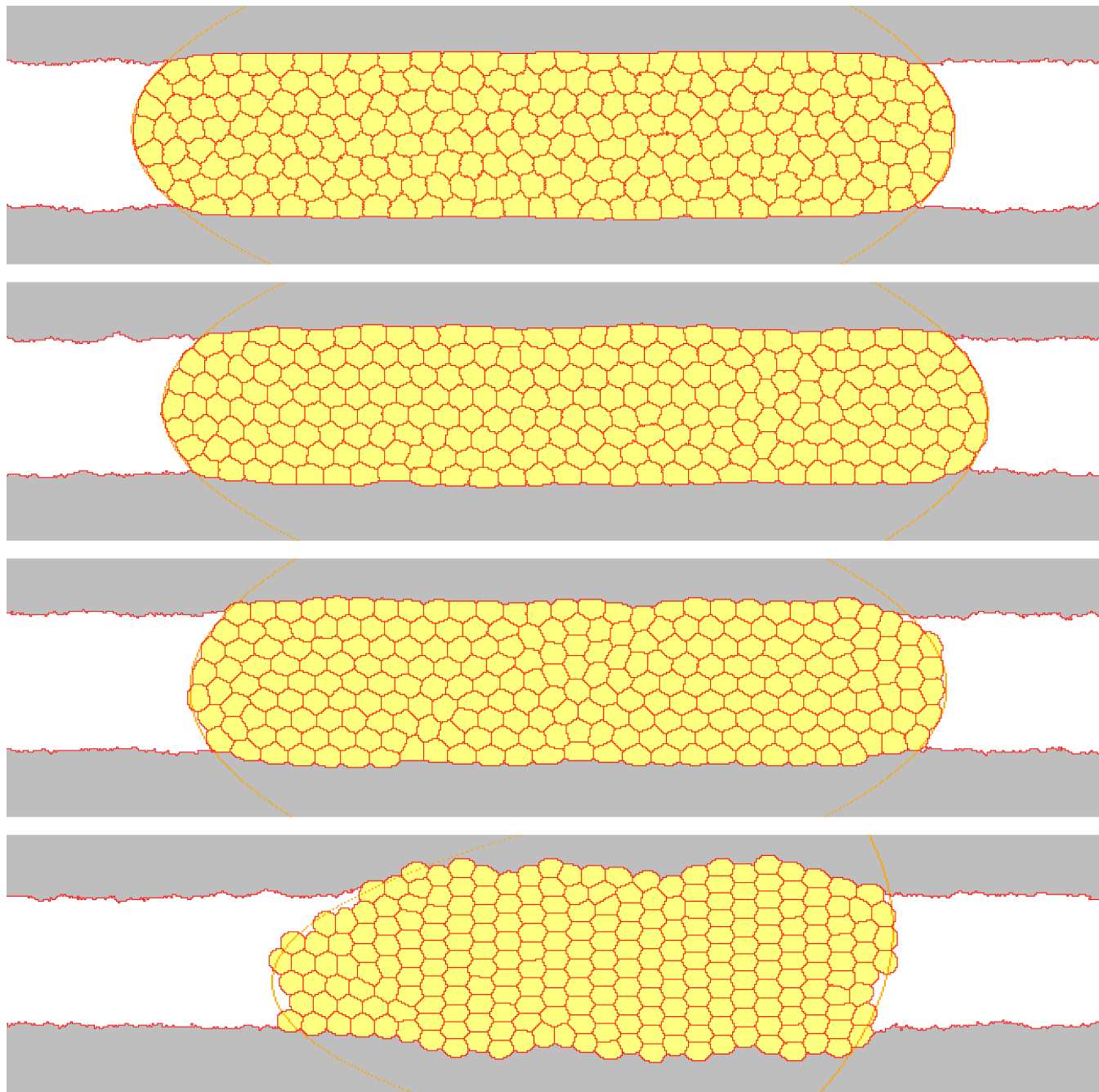
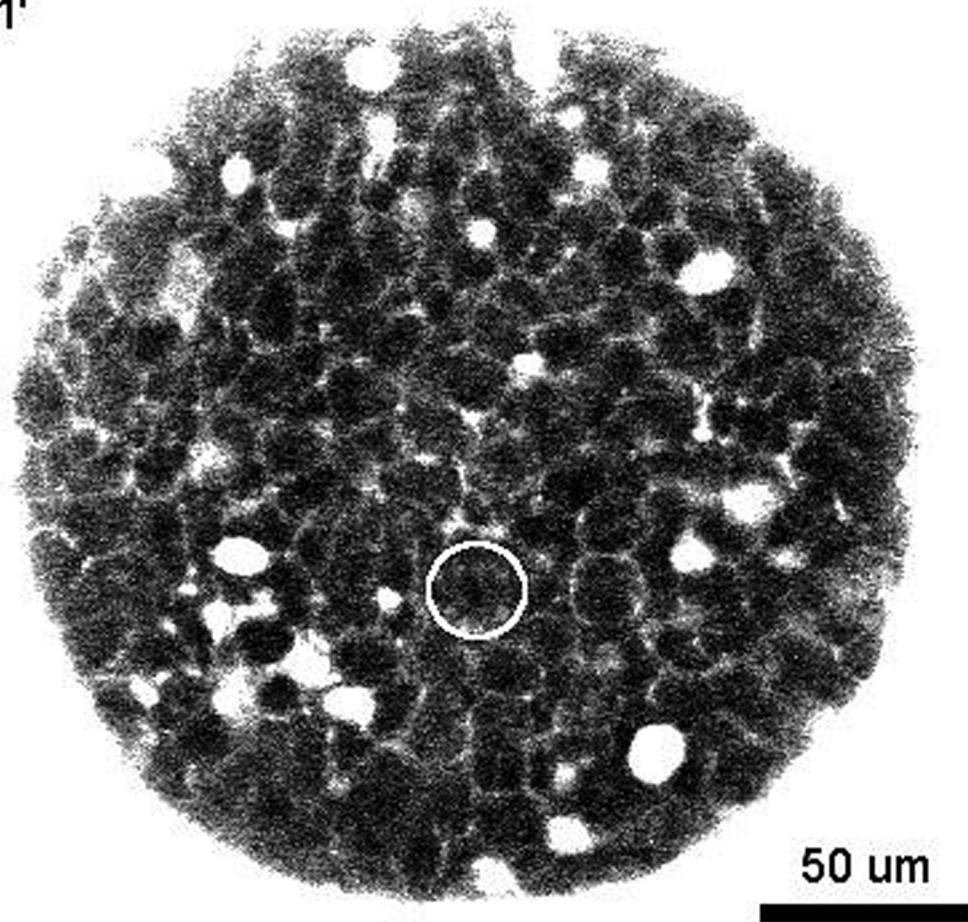


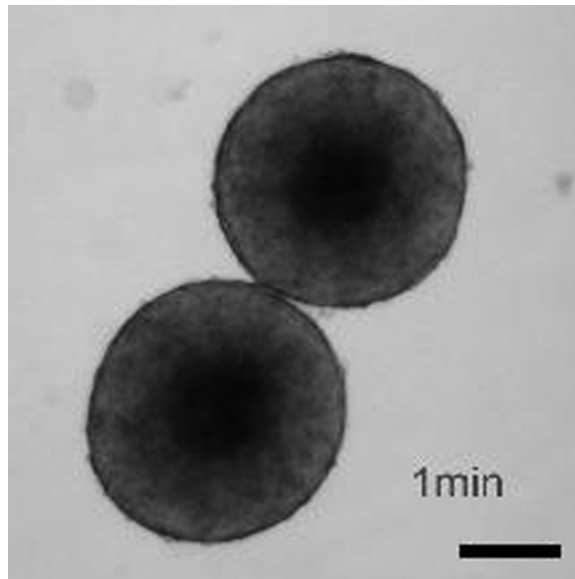
**Fig. S4.** Simulated aggregates with a liquid drop-like shape and deviations from it. Snapshots are taken at the end of simulations, after  $10^6$  Monte Carlo steps. From top to bottom, increasing values of cell–cell tension  $\gamma_{CC}$ :  $2.26 \times 10^5$ ,  $4.52 \times 10^5$ ,  $6.78 \times 10^5$  and  $11.07 \times 10^5$ . The force exerted on the plates increases, as is visible by the plate deformation. Equally, the cells are increasingly deformed, which indicates that more elastic energy is stored. The last image is an extreme example: The cell–cell tension  $\gamma_{CC}$  is large enough to dominate the fluctuation amplitude  $\xi$ , the aggregate surface tension  $\sigma$ , and the plate stiffness  $k$ .

1'



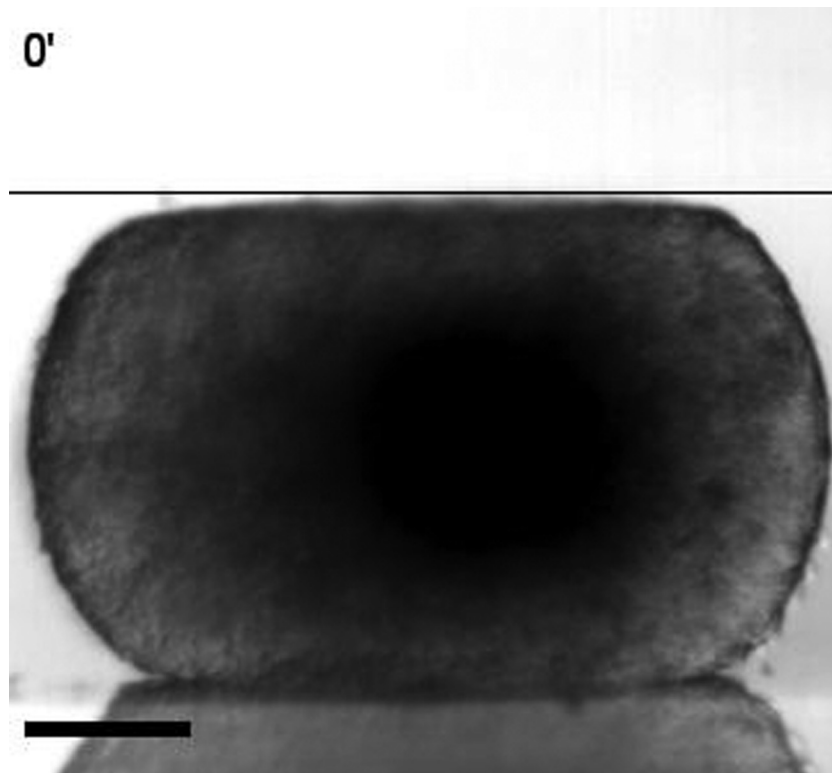
**Movie S1.** Two-photon microscopy of cell rearrangements. In this top view of the middle plane of an embryonic F9 aggregate compressed at a 27% compression rate, the extracellular space is visualized by the freely diffusible dye sulforhodamine B. The average aggregate diameter is 215  $\mu\text{m}$ . Images are taken every minute during 15 min. Contrast has been enhanced. On the first image, the white circle highlights a cell that leaves the plane of the image at  $t = 10$  min.

[Movie S1 \(AVI\)](#)



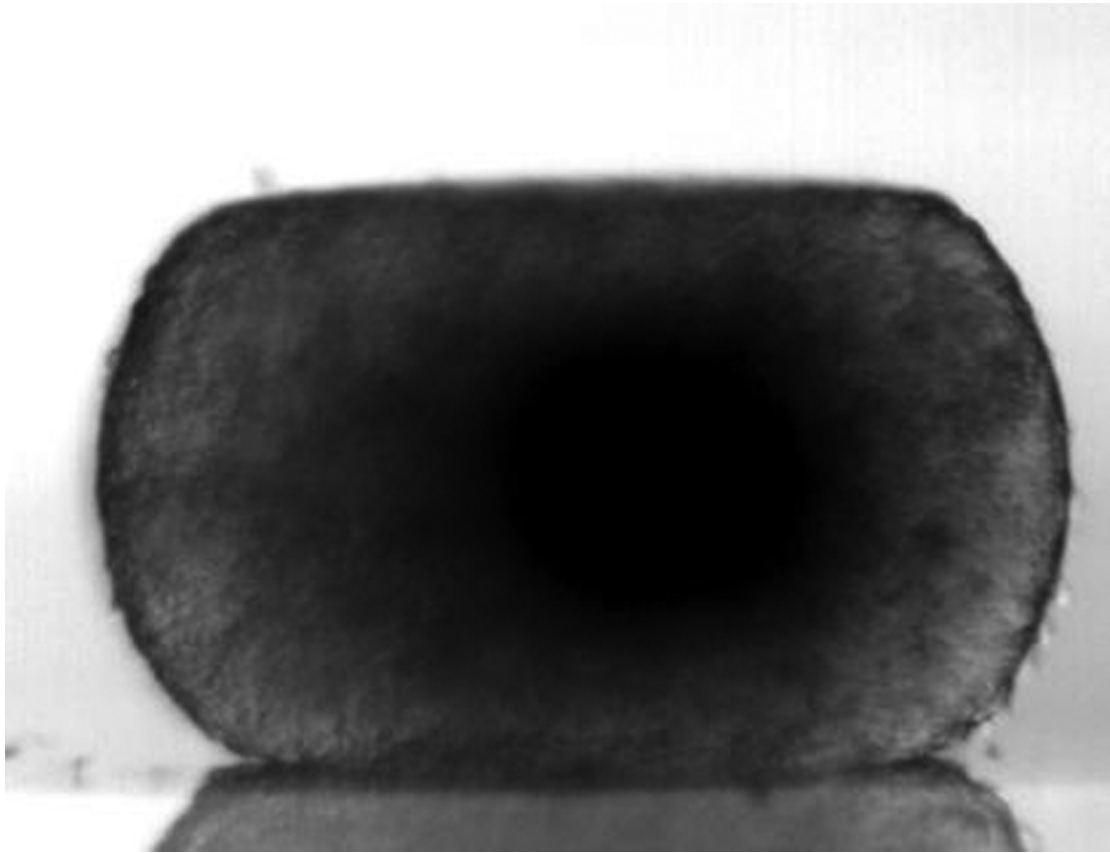
**Movie S2.** Fusion of two embryonic F9 aggregates. (Scale bar, 200  $\mu\text{m}$ .) Interval between two images: 15 min. Total duration: 255 min.

[Movie S2 \(AVI\)](#)



**Movie S3A.** Relaxation of an embryonic F9 aggregate. It has been compressed at  $\epsilon_{\text{comp}} = 0.3$  for  $t_{\text{comp}} = 60$  min, then left free to relax. (A) Complete relaxation. Total duration: 20 min. Interval between two images: 1 min. The solid line indicates the initial compression height. (Scale bar,  $100 \mu\text{m}$ .) (B) Same experiment, shown only during the first 70 s. Interval between two images: 1 s.

[Movie S3A \(AVI\)](#)



Movie S3B. Continued.

[Movie S3B \(AVI\)](#)